Food and Bioprocess Technology (2021) 14:1216–1230
https://doi.org/10.1007/s11947-021-02632-z

ORIGINAL RESEARCH

Analysis of the Adsorption and Release Processes of Bioactives from *Lamiaceae* Plant Extracts on Alginate Microbeads

Maja Benković[1] · Ivana Sarić[1] · Ana Jurinjak Tušek[1] · Tamara Jurina[1] · Jasenka Gajdoš Kljusurić[1] · Davor Valinger[1]

Received: 24 November 2020 / Accepted: 23 March 2021 / Published online: 31 March 2021

Abstract

Microencapsulation is a frequently used method for protection of functional properties of bioactives. In this study, alginate was used for microencapsulation of the bioactives from five *Lamiaceae* family plants: lavender, lemon balm, peppermint, sage, and thyme. Analysis of the adsorption and release processes of *Lamiaceae* bioactives on alginate microbeads was also performed. Based on the analysis of the extract used for the adsorption process, it was concluded that the highest amount of polyphenols (30% of the polyphenols contained in the extract) was transferred to the microbeads from the thyme extract. Also, a period of bead shrinkage during the adsorption process was detected which lasted until 30 min for thyme, 50 min for lavender, lemon balm, and peppermint, while the shrinkage for the sage extract lasted for 60 min. During the release process, a simultaneous rise of conductivity, total dissolved solids (TDS), polyphenolic (TPC), and antioxidant capacity values in the release media was detected at regular time intervals. The best suited model for the description of the release kinetics was the Korsmeyer-Peppas model, based on which it was concluded that the lemon balm polyphenols entrapped in the alginate matrix were released the fastest ($k = 0.326 \pm 0.048\ min^{-1}$) and that the release was governed by a pseudo-Fickian diffusion mechanism, since the calculated release exponent values (n) were lower than 0.5.

Keywords Alginate · Adsorption · Bioactives · Release kinetics · Modeling

Introduction

Self-grown medicinal plants have been known to cure or help prevent diseases since the ancient times. The *Lamiaceae* plant family is known as an abundant source of bioactives, which include phenolic compounds such as rosmarinic acid, carvacrol, tymol, and similar (Skendi et al. 2017). The above-mentioned compounds can successfully be extracted from *Lamiaceae* plants using different extraction methods (Jurinjak Tušek et al. 2016) and can be further stabilized for use in functional food production. There are several proposed ways to stabilize the bioactives during application, with most popular one being microencapsulation. Microencapsulation is a method of functionality preservation which puts a protective layer around the core which contains an active material in liquid, solid, or gaseous form (Bodade and Bodade 2020; Chen et al. 2019; Tarone et al. 2020). One of the most widely studied microencapsulation method is extrusion dripping, where microcapsules are produced from different polymers (alginate, chitosan, β-cyclodextrin, maltodextrin, gum Arabic, modified starch etc.) (Belščak-Cvitanović et al. 2011; Massounga Bora et al. 2018) which are passed through a syringe at a certain flow ratio to a receiving solution where ion exchange occurs causing the polymerization (Stojanović et al. 2012). Literature data on extrusion dripping includes examples of *Entada africana* leaf extract (Obidike & Emeje, 2011), raspberry leaf, hawthorn, yarrow, nettle and olive leaf extract (Belščak-Cvitanović et al. 2011), dandelion (Bušić et al. 2018), thyme (Stojanović et al. 2012), fish oil (Strobel et al. 2020), probiotic bacteria (Rodrigues et al. 2012; Shinde et al. 2014), chlorogenic acid (Gonçalves et al. 2017), and many more bioactive ingredients (Fangmeier et al. 2019). The microencapsulated bioactives can be produced in two ways: the first includes dissolving the shell material in the extract and then extruding the microbeads, and the second producing plain shell beads by extrusion and then immersing them into extracts to allow adsorption of the bioactive

✉ Ana Jurinjak Tušek
ana.tusek.jurinjak@pbf.unizg.hr

[1] Faculty of Food Technology and Biotechnology, University of Zagreb, Pierottijeva 6, 10000 Zagreb, Croatia

compounds. Those two preparation methods usually yield in different encapsulation efficiencies (Stojanović et al. 2012).

According to Fangmeier et al. (2019), sodium alginate is the most commonly used wall material in extrusion dripping. Its advantages include its biocompatibility, low toxicity, relatively low cost, and mild gelation by addition of divalent cations such as Ca^{2+} (Lee & Mooney, 2012). In the food industry, it has been used to coat fruits and vegetables, for microbial and viral protection and as a gelling, thickening, stabilizing, and emulsifying agent (Puscaselu et al. 2020). Some of its major advantages also include biodegradability and the capability to control the release of encapsulated bioactives and drugs from alginate matrices, which extends its application to pharmaceutical industry and medicine (Lee and Mooney 2012; Puscaselu et al. 2020). However, alginate tends to show a deterioration of protective properties when subjected to low pH values (Fangmeier et al. 2019). Since herbal extracts usually have slightly acidic pH, it is important to thoroughly analyze the behavior of alginate beads during adsorption of bioactives from acidic extracts. Another important factor to be considered during microencapsulation are the release profiles of the bioactives from the microbeads and a detailed kinetic analysis of the release process. Although there are examples of "in-depth" kinetic studies of bioactives release properties in literature (Ansarifar et al. 2017; Bucurescu et al. 2018; Dima et al. 2016; Jim et al. 2010; Stojanović et al. 2012), they were not done on alginate encapsulated *Lamiaceae* extract. In-depth release studies were mostly reserved for pharmaceutical preparations, where release rates and release mechanisms must be strictly defined. However, those kinetic parameters are equally important for microencapsulated bioactives.

Therefore, the aim of this study was to describe the adsorption and release processes of bioactives originating form five *Lamiaceae* plant extracts (lavender, peppermint, sage, thyme, and lemon balm). Furthermore, the study aimed to perform a detailed analysis of the release profiles using mathematical modeling tools, which would result in defined and comparable release rates of bioactives for five different *Lamiaceae* plant encapsulated extracts, as well as an insight in mechanisms which govern the release of plant bioactives from the produced alginate microbeads.

Materials and Methods

Materials

Plant Material

Herbal materials used in this research were sun dried ground *Lamiaceae* family plants: lavender (*Lavandula x hybrida* L.), lemon balm (*Melissa officinalis* L.), peppermint (*Mentha pipperita* L.), sage (*Salvia officinalis* L.), and thyme (*Thymus serpyllum* L.). Herbal material was acquired from a local manufacturer Suban d.o.o. (Strmec Samoborski, Croatia), originating from a flowering season of 2018, all having initial moisture content after drying below 15%.

Chemicals and Reagents

Trolox (6-hydroxy-2,5,7,8-tetra methylchromane-2-carboxylic acid), DPPH radical (1,1-diphenyl-1-picrylhydrazyl), TPTZ (2,4,6-tripyridyl-1,3,5-triazine), gallic acid (3,4,5-trihydroxybenzoic acid), iron (III) chloride hexahydrate, and iron (II) sulfate heptahydrate were obtained from Sigma–Aldrich Chemie (Steinheim, Germany). Ethanol (96%) was obtained from Carlo Erba Reagents (Cornaredo, Italy). Methanol was obtained from J.T. Baker (Deventer, Netherlands). Calcium chloride and sodium carbonate were obtained from Gram-Mol d.o.o. (Zagreb, Croatia). Folin-Ciocalteu reagent was obtained from Kemika d.d. (Zagreb, Croatia) and acetic acid from T.T.T. d.o.o. (Sveta Nedjelja, Croatia). Sodium alginate was purchased from Fisher Scientific (Loughborough, England).

Methods

Extract Preparation

An amount of 12 g of plant material was weighed and transferred into a 2-L glass beaker filled with 600 mL of distilled water heated to 80 °C. The prepared extraction mixture was thermostated at 80 °C in an oil bath (IKA HBR 4 digital, IKA-Werk, Staufen, Germany) at 250 rpm (rpm) for 30 min. After the extraction time has elapsed, the sample was filtered using a cellulose filter paper with pore size 5 to 13 μm (LLG Labware, Meckheim, Germany) and a Rocker 300 vacuum pump (Rocker Scientific Ltd., New Taipei City, Taiwan) to separate the aqueous extract from the solid phase. One part of the extracts were immediately used for microencapsulation and the other part was stored at −18 °C until further analysis.

Alginate Beads Preparation

First, a 3% (*w*/w) alginate solution is prepared by dissolving alginate in distilled water. The mixture was homogenized on a magnetic stirrer SB 162–3 (Stuart, Staffordshire, UK) and degassed in an ultrasound bath for 5 min (Uten, China). After degassing, the solution is transferred in a syringe with a 0.7-mm internal diameter (DB, Franklin Lakes, NJ) and mounted on a NE-300 piston pump (New Era Pump Systems, USA) with a flow rate of 1000 μL/min. The beads were collected in a glass beaker containing a 2% (w/w) $CaCl_2$ solution. After preparation, the beads were drained from the $CaCl_2$ solution, dried in a desiccator, and further used for adsorption.

Adsorption Profiles of the Extracts on Alginate Beads

Two types of the adsorption experiments were performed: (i) dynamic experiment with sampling at regular time intervals to obtain the adsorption profiles and (ii) experiment to determine the amounts of adsorbed bioactives after overnight ($t = 16$ h) adsorption. The dynamic experiment was performed by adding 30 g of beads to 450 mL of the extract solution at room temperature (23 °C). The mixture was then placed on a magnetic stirrer at 200 rpm and the samples of the beads (for determination of physical properties – weight and diameter) and 700 μm surrounding extract were taken in regular time intervals (0, 2, 4, 6, 8, 10, 15, 20, 30, 40, 50, 60, 70, 80, and 90 min). The volume of the samples taken was calculated to ensure that the change in total volume of the mixture was less than 10% which does not affect the solid to liquid ratio of the mixture beyond the point of the experimental error and is considered as a relatively constant volume of the batch (Jurinjak Tušek et al. 2016; Sudar et al. 2019). Beside the adsorption of the bioactives from extracts on the microbeads, a control experiment was also performed at the same conditions: 30 g of beads was added to 450 mL of distilled water, to ensure that the analyzed conductometric properties did not originate from the $CaCl_2$ solution used to make the beads. The weight and diameter of the beads and the conductometric properties of the extract samples and distilled water from the zero experiment were determined immediately after sampling. The samples taken at regular time intervals were used for the dynamic experiment, while the rest of the mixture containing the beads and the extract was left to stir overnight ($t = 16$ h) to determine the amounts of adsorbed bioactives after overnight adsorption at given conditions. After adsorption, the beads were drained from the mixture, washed with the extract solution, dried in a desiccator, and further analyzed (weight, diameter, dry matter, total polyphenol content, 1,1-diphenyl-1-picrylhydrazyl assay, ferric reducing antioxidant power assay).

Bead Diameter and Dry Matter Content

Bead diameter was measured using a caliper and the results were presented as mean ($N = 10$) ± standard deviation. Dry matter content was determined according to a previously described method by Jurinjak Tušek et al. (2020).

Conductometric Analysis

Conductometric analysis was performed using a SevenCompact conductometer (Mettler Toledo, Greifensee, Switzerland) by immersing the electrode in a liquid sample. Results were expressed as conductivity (μS/cm) and total dissolved solids (TDS, mg/L). All measurements were performed in triplicate.

Release Profiles

Release profiles of bioactive molecules from the alginate matrix were determined in distilled water as the solvent, at room temperature (23 °C) (Belščak-Cvitanović et al. 2011; Strobel et al. 2016; Strobel et al. 2020). An amount of 18 g of whole, undamaged beads with adsorbed extract was put in 105 mL distilled water on a magnetic stirrer set to 100 rpm. For the control experiment, 18 g of plain alginate beads was placed in 105 mL of distilled water. Samples of the solvent surrounding the beads (500 μL) were collected in regular time intervals (0, 2, 4, 6, 8, 10, 15, 20, 30, 40, 50, 60, 70, 80, and 90 min) and analyzed with respect to conductivity, total dissolved solids (TDS), and chemical analyses (total polyphenolic content (TPC), 1,1-diphenyl-1-picrylhydrazyl assay (DPPH) and ferric reducing antioxidant power assay (FRAP)). The volume of the samples taken was calculated to ensure that the change in total volume of the mixture was less than 10% which does not affect the solid to liquid ratio of the mixture beyond the point of the experimental error and is considered as a relatively constant volume of the batch (Jurinjak Tušek et al. 2016; Sudar et al. 2019).

Preparation of the Beads for Chemical Analysis

An amount of 1 g of beads was ground with a pestle and mortar and dissolved in 2 mL of distilled water at room temperature. The mixture was mixed vigorously for 10 min using a magnetic stirrer and transferred to a Falcon cuvette. The cuvette was then centrifuged at 6000 rpm (Hettich, Kirchlengern, Germany) to separate the sediment from the supernatant and the supernatant was used for further chemical analyses. The beads used for chemical analyses were the beads taken before the adsorption process and after the adsorption process was completely finished ($t = 16$ h).

Determination of Total Polyphenolic Content, Antioxidant Capacity by the DPPH and FRAP Methods

The total polyphenolic content (TPC) was determined spectrophotometrically using the Folin-Ciocalteu reagent, as previously described in studies by Singleton and Rossi (1965) and Jurinjak Tušek et al. (2020). The DPPH method was also carried out spectrophotometrically according to a method previously described by Brand-Williams et al. (1995) and Jurinjak Tušek et al. (2020). The FRAP (Ferric ion reducing antioxidant power) assay was conducted according to a method by Benzie and Strain (1996). All measurements were done in triplicate.

Encapsulation Efficiency

The encapsulation efficiency (EE) was calculated for TPC according to Eq. (1):

$$EE\ (\%) = \frac{M_0 - M_t}{M_0} \quad (1)$$

where M_0 represents the TPC of the extract before encapsulation, and M_t represents the TPC of the extract after encapsulation.

TPC Stability

The TPC stability was determined using a mass balance analysis (Eq. (2)) previously described by Chan et al. (2010):

$$\text{Sum of TPC mass fractions} = \left(\frac{m_{\text{TPC,beads}}}{m_{\text{TPC,0}}}\right) + \left(\frac{m_{\text{TPC,residual}}}{m_{\text{TPC,0}}}\right) \quad (2)$$

where $m_{\text{TPC,beads}}$ represents the mass of total polyphenols in beads (mg), $m_{\text{TPC},0}$ represents the mass of total polyphenols in the original extract before adsorption (mg), and $m_{\text{TPC,residual}}$ represents the mass of total polyphenols in the extract after adsorption (mg). Based on this equation, the mass ratio of TPC in the beads and in the residual extract can be determined. Furthermore, if the sum of two fractions is about one, there was no significant loss in TPC stability during the adsorption process (Chan et al. 2010).

Microscopic Analysis of the Microbeads

The microbeads' surface and cross-sections were analyzed using a light microscope (Motic B series, Motic, Barcelona, Spain) at × 4 magnification, coupled with a Moticam 3 series camera with a CMOS sensor, a 16-mm focusable lens, and a 3-MB capture resolution. The microscales were added to the micrographs using a build in Motic Images Plus 2.0. software (Moticam, Barcelona, Spain).

Statistical Analysis and Polyphenol Release Kinetics Modeling

Statistical analysis of the experimental data was performed using the Statistica v.13 software (Tibco Statistica, Palo Alto, USA), using the *t*-test for independent samples to detect differences among values at $p < 0.05$. Fitting of the experimental data to mathematical models was also done using the same software package, according to the mathematical models previously described in the literature (Cortés-Camargo et al. 2019; Rezaei and Nasirpour 2019). Models used are shown in Table 1.

Table 1 Mathematical models used for estimation of release kinetics

Model	Equation
Zero-order kinetic model	$M_t = kt$
First-order kinetic model	$M_t = M_0 e^{-kt}$
Korsmeyer-Peppas	$M_t = kt^n$
Higuchi	$M_t = kt^{0.5}$

Parameters assessed by the models were k – release rate (min^{-1}), M_t – concentration of polyphenols (TPC) in the release medium (water) at time t, M_0 – concentration of polyphenols (TPC) in the release medium (water) at time $t = 0$ and n is the release exponent that describes the release mechanism: $n < 0.5$, a pseudo-Fickian diffusion mechanism; $n = 0.5$ a Fickian mechanism; $0.5 < n < 1$, an anomalous diffusion mechanism; and for $n = 1$, a non-Fickian diffusion mechanism (Rezaei and Nasirpour 2019). Data used for the models were the experimental values for TPC, as a representation of the concentration of a certain compound (or group of compounds) in the extract. Adequacy of the developed models was assessed based on the determination coefficients (R^2) and the root mean squared error values (RMSE).

Results and Discussion

Analysis of the Extracts before and after Adsorption on Alginate Beads

Physical and chemical properties of the extracts produced by adsorption of bioactives on alginate beads before and after the adsorption process are shown in Table 2.

The TDS and the conductivity, as two interconnected values which can be determined by using the conductometric electrode, ranged from 482 ± 5 mg/L for sage to 793 ± 16 mg/L for lemon balm (for TDS), and from 998 ± 10 for sage to 1568 ± 15 μS/cm for lemon balm (for conductivity, Table 2). It can be seen that lemon balm contained the highest amount of water soluble bioactives which contributed to the increase of conductivity of the extracts and was followed by peppermint, lavender, thyme, and sage (in a decreasing order). Also, the lowest values of TDS and conductivity were determined for the control experiment (distilled water) (TDS = 2.0 ± 0.5 mg/L and conductivity = 125 ± 3 μS/cm, respectively). TDS and conductivity analysis as a mean of monitoring the extraction process was previously described by Jurinjak Tušek et al. (2016) and Jurinjak Tušek et al. (2018), while Saad et al. (2015) concluded that electrical conductivity can be used as a method to predict antioxidant properties of herbal extracts. In a study by Jurinjak Tušek et al. (2018), it was reported that the highest conductivity values were also acquired for the lemon balm extracts, which ranged from approximately 850 to

Table 2 Physical and chemical properties of aqueous *Lamiacae* plant extracts before and after overnight ($t = 16$ h) adsorption on alginate beads. Results are expressed as mean ($n = 3$) ± SD (n.d. stands for "not detected"). Values in brackets represent the encapsulation efficiency calculated based on the concentration of polyphenols (TPC) in the extract before and after encapsulation. Different superscript letters in the columns represent values with significant differences at $p < 0.05$

Plant	TDS mg/L)	Conductivity (μS/cm)	Dry matter (extraction yield) (%)	pH	TPC (mg GAE/g d.m.)	DPPH (mmol Trolox/g d.m.)	FRAP (mmol $FeSO_4$ $7H_2O$/g d.m.)
Before adsorption							
Lavender	592 ± 12^a	1171 ± 12^a	0.513±0.008^a	4.96 ± 0.10^a	24.5±3.0^a	0.258±0.019^a	0.479±0.002^a
Lemon balm	793 ± 16^b	1568 ± 15^b	0.692±0.010^b	5.86 ± 0.04^b	79.9±1.9^b	0.624±0.023^b	0.874±0.009^b
Peppermint	607 ± 5^c	1246 ± 17^c	0.657±0.016^c	6.18 ± 0.05^c	57.0±1.3^c	0.520±0.047^c	0.588±0.029^c
Sage	482 ± 5^d	998 ± 10^d	0.540±0.049^a	5.78 ± 0.03^d	56.4±3.2^c	0.457±0.010^d	0.696±0.033^d
Thyme	508 ± 10^d	1002 ± 10^d	0.398±0.008^d	6.05 ± 0.05^e	42.3±0.6^d	0.393±0.002^e	0.547±0.037^e
Distilled water (control)	2.0 ± 0.5^e	125 ± 3^e	n.d.	6.69 ± 0.01^f	n.d.	n.d.	n.d.
After adsorption							
Lavender	906 ± 11^a	1838 ± 14^a	0.430±0.026^a	5.02 ± 0.10^a	21.8±2.6^a (11%)	0.197±0.003^a	0.339±0.009^a
Lemon balm	1081 ± 22^b	2190 ± 16^b	0.658±0.035^b	6.01 ± 0.05^b	65.5±1.9^b (18%)	0.608±0.006^b	0.750±0.061^b
Peppermint	870 ± 8^c	1723 ± 11^c	0.647±0.035^b	6.05 ± 0.05^b	50.2±1.9^c (12%)	0.298±0.016^c	0.575±0.019^c
Sage	940 ± 8^d	1870 ± 22^d	0.529±0.009^c	5.84 ± 0.04^c	51.8±2.2^c (9%)	0.401±0.005^d	0.643±0.015^d
Thyme	743 ± 6^e	1544 ± 13^e	0.353±0.033^d	6.20 ± 0.05^d	29.6±3.2^d (30%)	0.261±0.014^e	0.333±0.004^a
Distilled water (control)	3.6 ± 0.3^f	249 ± 2.828^f	n.d.	6.40 ± 0.02^f	n.d.	n.d.	n.d.

1900 μS/cm, depending on the experimental conditions used for extract preparation. The experimental conditions from the study by Jurinjak Tušek et al. (2018) which are the most similar to this study are $t = 30$ min, $T = 80$ °C, and 750 rpm, where slightly higher conductivity values were detected, which was due to a greater mixing speed (750 rpm compared to 250 rpm in this study). The dry matter content of the extracts before adsorption ranged from 0.398 ± 0.008% for thyme to 0.692 ± 0.010% for lemon balm. Similar values were reported in studies by Oreopoulou et al. (2018) and Fornari et al. (2012) for hydrodistillation and supercritical CO_2 extraction of bioactives from the *Lamiaceae* plants. pH values of the extracts before adsorption ranged from 4.96 ± 0.10 (lavender) to 6.18 ± 0.05 (peppermint), indicating a slight acidity of all the extracts.

The *Lamiaceae* plants produce a wide spectrum of bioactive compounds (flavonoids, terpenoids, phenolics, and alkaloids), and have proven biological activities (Marchioni et al. 2020). The five plants chosen for this research are widely cultivated, available, and often used in Croatia in form of teas or nutritional supplements. Based on the data shown in Table 2, the highest TPC was detected for lemon balm extract (79.9 ± 1.9 mg GAE/g d.m.), followed by peppermint (57.0 ± 1.3 mg GAE/g d.m.), sage (56.4 ± 3.2 mg GAE/g d.m), thyme (42.3 ± 0.6 mg GAE/g d.m), and lavender (24.5 ± 3.0 mg GAE/g d.m). The same trend was detected for the antioxidant capacity determined by the DPPH method, with slight differences for the FRAP method, where sage exhibited a slightly higher antioxidant capacity compared to peppermint, but those differences were within the margin of error (standard deviation). According to Matkowski and Piotrowska (2006), the phenolics extracted from the members of *Lamiaceae* plant family have been reported to be very efficient antioxidants and free radical scavengers. However, Dorman et al. (2003) emphasized that antioxidant scavenging characteristics are not fully related to the total phenolic contents of the extracts and presumed that the scavenging action was dependent on rosmarinic acid, the major phenolic component present in this type of *Lamiaceae* extract. A further study by Belščak-Cvitanović et al. (2018), revealed that the five *Lamiaceae* plants used in this study differ on the content of the predominant group of polyphenols: phenolic acids (hydroxycinnamic acids, HcA) and flavonoids (flavons and flavonols). These results showed that peppermint was characterized by the highest content of HcA, followed by lemon balm, lavender, thyme, and sage. In the case of flavons and flavanols, the highest values were once again detected for peppermint, followed by sage, thyme, lemon balm, and lavender.

The conductometry data after adsorption revealed an increase in TDS and conductivity values in comparison to the values measured before adsorption for all analyzed extracts, including the control experiment. It would be logical to expect

a decrease in those values, since some of the bioactives have left the extract and have been adsorbed to the alginate microbeads. However, the explanation offered in this case is connected to the $CaCl_2$ solution used to receive the beads. Namely, some parts of the $CaCl_2$ ions were apparently left on the surface of the alginate microbeads, which diffused into the extract during adsorption and hence caused an increase in conductivity and TDS values (Pham and Fulton 2013). Based on the data for the control experiment (distilled water) before and after adsorption, with an assumption that the rise in conductivity and TDS is indeed connected to the $CaCl_2$ ions originating from the beads, it can be seen that the difference in conductivities and TDS of distilled water before and after adsorption results in 1.6 mg/L and 124 μS/cm, respectively. This data should be deducted from the values of TDS and conductivity determined for the extracts prior to and after adsorption to get a precise insight into the real values for the extracts. The highest TDS and conductivity values were detected for the lemon balm extracts, and the lowest for the sage and thyme extracts. The differences in TDS and conductivity values of the extracts have previously been documented in studies by (Saad et al. 2015; Jurinjak Tušek et al. 2018), and can be attributed to the differences in the composition of the bioactives of a certain plant and their ability to produce ions in solutions which can conduct electrical current.

The dry matter content of the extracts after adsorption dropped compared to the values recorded before adsorption. The dry matter data does not necessarily correlate with TDS and conductivity, since it cannot include the ions which contribute to conductivity. Namely, the increase in conductivity was noticed after adsorption and contributed to $CaCl_2$ ions. This also caused a rise in TDS, since the two values are linearly correlated based on the equation TDS = k·conductivity, with k values ranging from 0.5 to 0.75 depending on the type of water used for the extraction (Rusydi 2018). TDS includes dissolved organic and inorganic substances present in either molecular, suspended, or ionized form. Dry matter, on the other hand, does not include the ions. Therefore, the fall in dry matter is an indication that the bioactives have indeed transferred from the extract to the beads, while the TDS additionally indicated that, besides the mass transfer, a transfer of ions from the beads to the extract occurred resulting in an extract which contained a lot of ionized matter after the adsorption process. pH values increased slightly after adsorption, which could be an indication that the acidic bioactives were transferred from the extract to the alginate beads. The TPC content and the antioxidant capacities of the extracts measured by the DPPH and the FRAP method after adsorption also dropped. The lowest TPC content after adsorption was detected for the lavender extract (21.8 ± 2.6 mg GAE/g d.m.), and the highest for the lemon balm extract (65.5 ± 1.9 mg GAE/g d.m.). However, the highest amount of TPC was transferred to the beads from the thyme extract (30%) and the lowest from the sage extract (9%). The encapsulation efficiencies for the TPC were lower than those obtained in other studies, with an emphasis that the encapsulating material used in those studies did not contain the same amount of alginate in the solution (Stojanović et al. 2012). Also, it was noticed that the difference in TDS and conductivity prior to and after adsorption is inversely proportional to the EE – higher EE (based on the TPC content) is achieved in samples which have a smaller difference in TDS and conductivity values before and after extraction. We must emphasize that this correlation has to be further explored in order to acquire a plausible explanation for it, since the extracts used in this research are actually a complex combination of different bioactive molecules.

Adsorption Profiles

Adsorption process was monitored as a change in bead diameter when immersed into the extract and the change in the extract conductivity. Control experiment was also conducted for plain beads immersed into distilled water. Results are shown in Fig. 1.

In the case of plain beads (Fig. 1(a)), a slight variation in the bead diameter was recorded, but all the values were in the standard deviation (SD) range, and it was therefore considered that there was no significant change in the bead diameter during the adsorption process. Small differences in the diameter seen in Fig. 1 (a) can be a result of slight variations in bead diameter during production, when exiting the syringe tip. However, there was a change in the conductivity values of the surrounding release medium (water), which rose from the initial value of 11.5 μS/cm to the final 1107 μS/cm. It is evident from the results of the control experiment that a change in conductivity will occur during the adsorption process even if plain beads are used in distilled water. This conductivity has to be taken in account during analysis of the adsorption of the extracts, since it may give a false understanding that there are more bioactives in the extract. We propose a control experiment to be done every time a polar solvent is used, and the results from the control experiment to be deducted from the values obtained from the experiments where the extract was used. For beads immersed into the extracts, a different trend was discovered: immediately after immersion into the extract, alginate beads showed a decrease in diameter. The shrinkage period was considered to last until the first diameter larger than the initial one (3.306 ± 0.170 mm) was recorded for the tested beads. For lavender (Fig. 1(b)), the initial diameter was enlarged from 3.308 mm to the final value of 3.8 mm, with the first increase in diameter above the initial value detected at $t = 50$ min. At $t = 50$ min, the recorded conductivity value was 1382 μS/cm. Overall values of conductivity of the surrounding medium for lavender release changed from 1244 to 1380 μS/cm. For lemon balm (Fig. 1(c)), the

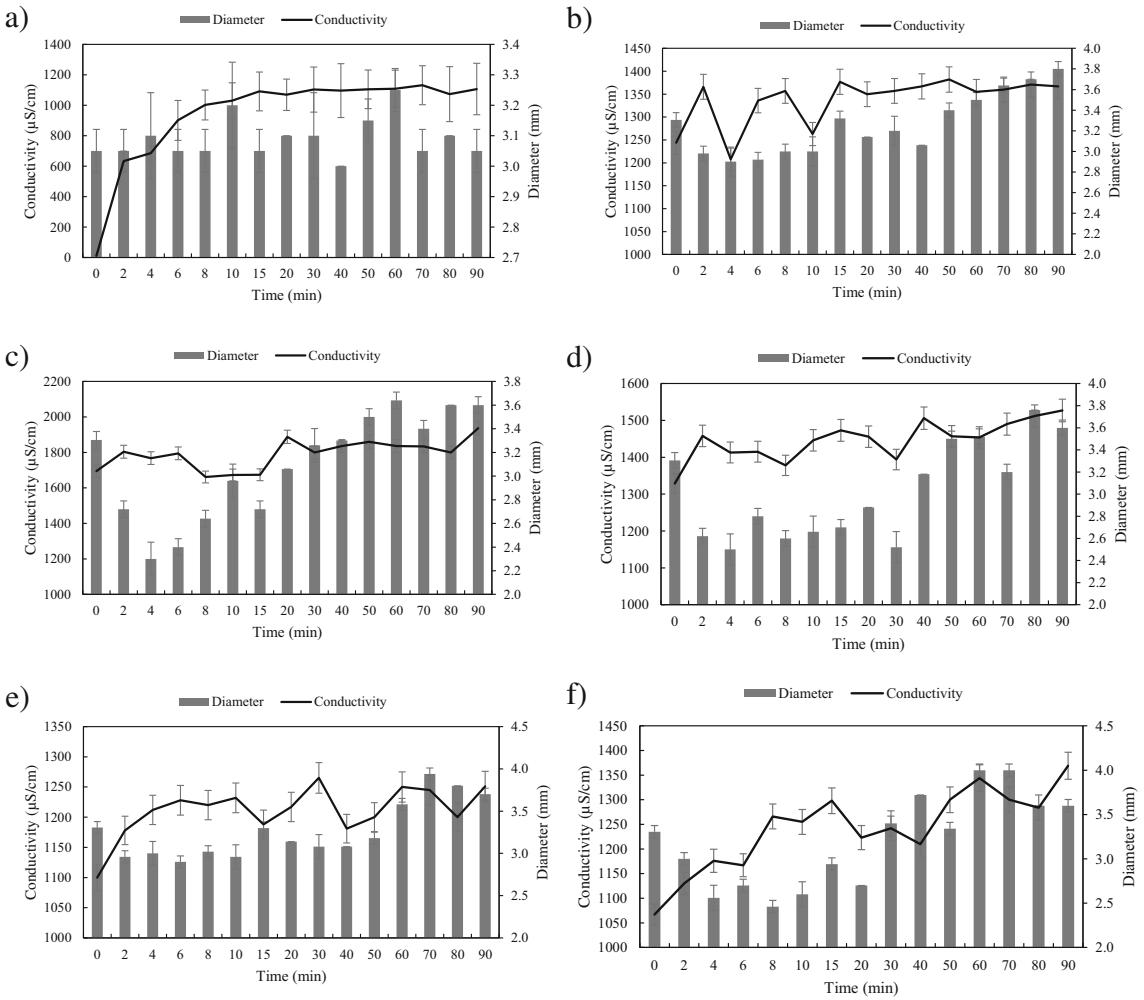

Fig. 1 Adsorption profiles of *Lamiaceae* plant extracts on alginate microbeads shown as a change in bead diameter and conductivity of the extract used for adsorption: (**a**) plain alginate beads, (**b**) lavender, (**c**) lemon balm, (**d**) peppermint, (**e**) sage, (**f**) thyme

initial diameter changed from 3.308 to 3.6 mm, with the first increase in diameter above the initial value detected also at $t =$ 50 min. At $t = 50$ min, the recorded conductivity value for lemon balm was 1836 μS/cm. Overall values of conductivity of the surrounding medium for lemon balm release changed from 1695 to 1937 μS/cm. For peppermint (Fig. 1(d)), the initial diameter was enlarged from 3.308 mm to the final value of 3.6 mm, with the first increase in diameter above the initial value detected at $t = 50$ min. At $t = 50$ min, the recorded conductivity value was 1457 μS/cm. Overall values of conductivity of the surrounding medium for peppermint release changed from 1329 to 1527 μS/cm. For sage (Fig. 1(e)), the initial diameter was enlarged from 3.308 mm to the final value of 3.7 mm, with the first increase in diameter above the initial value detected at $t = 60$ min. At $t = 60$ min, the recorded conductivity value was 1250 μS/cm. Overall values of conductivity of the surrounding medium for sage release changed from 1100 to 1527 μS/cm. For thyme (Fig. 1(f)), the initial diameter was enlarged from 3.308 mm to the final value of 3.6 mm, with the first increase in diameter above the initial value detected at $t = 30$ min. At $t = 30$ min, the recorded conductivity value was 1242 μS/cm. Overall values of conductivity of the surrounding medium for thyme release changed from 1067 to 1369 μS/cm. As seen in Fig. 1, the shrinkage period of the beads after they have been immersed into the extract was the longest for sage ($t = 60$ min), followed by lavender, lemon balm, and peppermint ($t = 50$ min) and thyme ($t =$ 30 min). It was also noticed that for lavender, lemon balm, and peppermint, the change of the initial conductivity values at which bead enlargement commenced was 138, 141, and 128 μS/cm, respectively. For sage the bead enlargement started after the conductivity rose by 150 μS/cm, and for thyme after a rise by 175 μS/cm. Based on the results displayed above, it is visible that the period of shrinkage is connected to the change in conductivity values, for which we can presume are dependent on the composition of the extracts. As argued before, the selected plants differ by the contents of the predominant group of polyphenols: phenolic acids (hydroxycinnamic acids, HcA) and flavonoids (flavons and flavonols), which can cause the detected differences in

conductivity (Belščak-Cvitanović et al. 2018). However, we must emphasize that this claim still has to be corroborated by future research. These results are of great importance, since they reveal the existence of a period of bead shrinkage before the extract is actually adsorbed on the bead. It is our opinion that this phase can be shortened or avoided by controlling the properties of the extract, or adapting the alginate concentration used for microencapsulation. Saitoh et al. (2000) discussed that the dimensional changes in alginate impressions in solutions are caused by physical and chemical interactions between solutions and alginate gels. The changes in bead volume and size were a result of osmotic pressure difference between the beads and the extract. According to Saitoh et al. (2000), the solvent in the gel may move into the solution in order to cancel out the osmotic pressure difference, leading to gel concentration. This drives the diffusion until equilibrium is attained. Montanucci et al. (2015) observed that microcapsules stored in saline shrank during 7 months of storage and attributed the shrinkage to a Gibbs-Donnan equilibrium, which is a passive equilibrium, peculiar to semipermeable membranes, that it is set up by negative charges of the alginates hydrogel carboxyl group not involved in cooperative binding of counterions in the junction zones of the network. Furthermore, in a review paper by Fangmeier et al. (2019), the authors state that sodium alginate gel as a wall material shrinks under acidic conditions due to the stretching of the carboxyl groups.

Furthermore, an interesting observation was seen for the adsorption process of plain beads and all 5 plants. It would be logical to expect that during the adsorption process, when the bioactives are adsorbed on the beads that the conductivity and TDS values of the extract in which the beads are immersed, to start to decrease. This research exhibited the opposite: as the adsorption process took place, a rise in conductivity values were detected. The rise was an indication that, besides the adsorption of bioactive, an exchange of ions between the beads and the extract also took place. As mentioned earlier, some parts of the $CaCl_2$ ions were apparently left on the surface of the alginate microbeads, which diffused into the extract during adsorption and hence caused an increase in conductivity and TDS values (Pham and Fulton 2013).

Although the adsorption kinetics of the extracts onto the alginate beads were not modeled in this study, a review of literature data suggests that the modeling could be done using the shrinking core model (SCM), which describes the adsorption as a diffusion process of the adsorbate through a spherical shell (Dominguez et al. 2019).

Physical and Chemical Properties of the Microbeads

After the adsorption process ($t = 16$ h), the beads' physical and chemical properties were analyzed. As a control sample, plain alginate beads were dissolved in distilled water and analyzed using the same methods as the beads containing the bioactives from herbal extracts. Results are shown in Table 3.

Physical properties of plain alginate beads before the adsorption process revealed that the average weight of the beads was 0.022 ± 0.002 g and the mean diameter 3.31 ± 0.17 mm (Table 3). After adsorption, weight of the beads increased to 0.030 ± 0.004 g (lavender and sage) and 0.34 ± 0.002 g (peppermint and thyme), which was a significant increase ($p < 0.05$) in comparison to the initial weight of the beads. The bead diameter also increased significantly ($p < 0.05$), indicating a swelling of alginate beads from initial 3.31 ± 0.17 mm to 4.00 ± 0.09 mm detected for thyme. The interactions between herbal extracts and the alginate beads and its effects on the encapsulation efficiency were studied by Chan et al. (2010) who concluded that high mannuronic acid content alginate beads swell to a larger volume after the adsorption process and result in a higher encapsulation efficiency, which was explained by a high content of biochemical agents in herbal extracts which can act as chelating agents. Alginate swelling has also previously been described in a study by Bajpai and Sharma (2004), who concluded that the swelling of alginate beads is dependent on the type of alginate used, pH values, and the presence of ions in the medium. In this case, beads immersed in the extract with the highest conductivity value (lemon balm) showed the smallest change in diameter, while the beads immersed in the extracts with the lowest conductivity showed the highest change in diameter (sage and thyme) (Tables 2 and 3), indicating an inversely proportional relationship between conductivity and diameter. The TPC content after microencapsulation is expressed per gram beads, and ranges from 0.59 ± 0.02 mg GAE/g beads for lemon balm to 0.19 ± 0.04 mg GAE/g beads for lavender. Results for the antioxidant capacity by the DPPH method showed that the highest amount of antioxidants was entrapped in the sage beads (3.46 ± 0.01 μmol Trolox/g beads), and the lowest in lavender beads (0.85 ± 0.04 μmol Trolox/g beads). For the FRAP method, results for the minimal amount of antioxidants entrapped in the alginate matrix were also detected for the lavender microbeads (1.18 ± 0.02 μmol $FeSO_4\ 7H_2O$/g beads), while the highest amount of antioxidants was detected in sage beads (2.83 ± 0.03 μmol $FeSO_4 \cdot 7H_2O$/g beads). Compared to the data shown in Table 2 for extracts after microencapsulation, some differences can be seen which were caused by the preparation procedure for microbeads' chemical analysis: some parts of the polyphenols and antioxidants were left bound on the alginate part (the sediment) after which was discarded after centrifugation, and thus the smaller amount of those compounds was detected in the microbeads. This can be confirmed by the calculated mass fractions of TPC present in the beads and in the residual extract. Namely, the portion of TPC which was adsorbed into the beads ranged from 0.007 (peppermint and thyme) to 0.01 (sage), while the mass fractions of TPC in the extract after adsorption ranged from 0.71

Table 3 Physical and chemical properties of microcapsules after the adsorption process (t = 16 h). Results for dry matter, TPC, and FRAP are expressed as mean (n = 3) ± SD, while the results for weight and diameter are expressed as mean (n = 10) ± SD (n.d. stands for "not detected"). Different superscript letters in the columns represent values with significant differences at $p < 0.05$

Plant	Weight (g)	Diameter (mm)	TPC (mg GAE/g beads)	Mass fraction of TPC in beads	Mass fraction of TPC in the residual extract	DPPH (μmol Trolox /g beads)	FRAP (μmol $FeSO_4$ $7H_2O$/g beads)
Alginate beads	0.022 ± 0.002^a	3.31 ± 0.17^a	n.d.	n.d.	n.d.	n.d.	n.d.
Lavender	0.030 ± 0.004^b	3.80 ± 0.10^b	0.19±0.04^a	0.008±0.001^a	0.89±0.06^a	0.85±0.04^a	1.18±0.02^a
Lemon balm	0.033 ± 0.002^b	3.64 ± 0.12^c	0.59±0.02^b	0.008±0.001^a	0.82±0.03^a	2.27±0.01^b	2.46±0.01^b
Peppermint	0.034 ± 0.002^c	3.76 ± 0.06^b	0.37±0.01^c	0.007±0.001^a	0.88±0.01^a	3.23±0.03^c	2.08±0.07^c
Sage	0.030 ± 0.004^b	3.94 ± 0.04^d	0.51±0.02^d	0.010±0.001^b	0.92±0.01^b	3.46±0.01^d	2.83±0.03^d
Thyme	0.034 ± 0.004^b	4.00 ± 0.09^d	0.25±0.01^e	0.007±0.001^a	0.71±0.02^c	1.88±0.04^e	1.57±0.02^e

to 0.92. This could be an indication of an aggravated mass transfer between the beads and the extract. However, the sum of the two mass fractions is close to 1, which indicated that the adsorption process did not cause a significant degradation of polyphenols.

Microscopic Analysis of the Beads

Micrographs of the beads made using a Motic light microscope are shown in Fig. 2.

As seen in Fig. 2, the beads appear to be spherical, and the surface of the plain microbeads (Fig. a1) appears to be smoother in comparison to the surface of the beads with adsorbed extract (Figs. b1–f1). The surface of the microbeads with the adsorbed extract has some irregularities and surface dents. However, the presence of big pores or any difference in pore size on a single bead or on all beads in comparison is not visible. In a study by Stojanović et al. (2012), SEM inspection of the alginate microbeads also revealed that the beads were spherical with a relatively smooth surface, but after microencapsulation of the thyme extract, a change in the surface structure was visible, resulting in a honeycomb-like surface. Furthermore, a study by Belščak-Cvitanović et al. (2015) also characterized plain alginate (2 or 3%) beads as the most regular, with a spherical shape and the straightest surface. In order to get an insight into the thickness of the outer layer, a cross-section of all the beads has also been photographed. As seen in the cross-section images (Figs. a2–f2), there are no visible differences in the thickness of the wall layer in among the beads with the adsorbed extract, which is a logical finding, since all the beads used for adsorption were produced from the same alginate solution. Some irregularities can be seen in Fig. a2 (plain bead cross-section) and Fig. c2 (lemon balm bead cross section) which were a result of bead tear during cross sectioning.

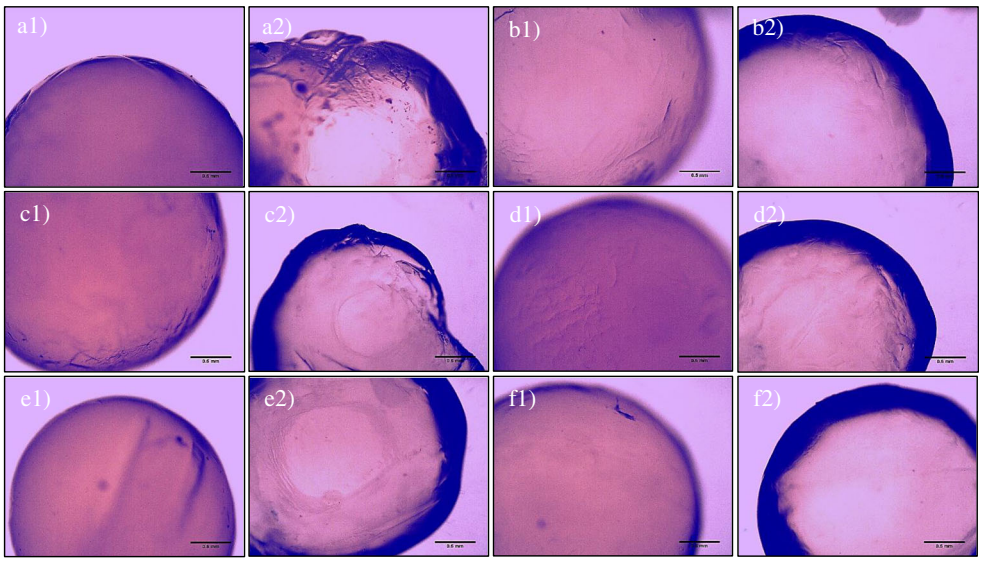

Fig. 2 Microscopic images of the beads at × 4 magnification: (a1) plain bead surface, (a2) plain bead cross section, (b1) lavender surface, (b2) lavender cross section, (c1) lemon balm surface, (c2) lemon balm cross section, (d1) peppermint surface, (d2) peppermint cross section, (e1) sage surface, (e2) sage cross-section, (f1) thyme surface, (f2) thyme cross section. The micro scale is presented for length of 0.5 mm

Analysis of the Release Profiles

Results for bioactives release profiles are presented in Fig. 3.

Conductometric analysis data is visible in Fig. 3 (a) (conductivity) and Fig. 3 (b) (TDS). Since those two parameters are connected, it is visible that both of them follow the same rising trend with passed time. The highest values of conductivity after 90 min of release testing were detected for the sage microbeads (491 μS/cm), and the lowest for the peppermint beads (342 μS/cm) (Fig. 3(a)), while the highest value of TDS after 90 min was detected for sage microbeads (245 mg/L), and the lowest for lavender microbeads (200 mg/L) (Fig. 3(b)). For the control experiment, the values after 90 min for TDS and conductivity were 124.5 mg/L and 249 μS/cm, respectively. It can be seen that the solvents' TDS and conductivity amounts to approximately 50% of the total conductivity determined for microbeads containing herbal extracts during the release process. Therefore, it must be emphasized again that, a thorough conductometric analysis of the solvent used for extraction must be performed prior to the analysis of the extracts, since the lack of solvent analysis can lead to false results and a presumption of a higher amount of bioactives than which is actually present in the beads during the release process. The TPC release profiles (Fig. 3(c)) revealed that the highest amount of polyphenols was released from the lemon balm extracts (TPC = 1.5 mg GAE/g beads at $t = 90$ min) and the lowest amount from lavender (TPC = 0.6 mg GAE/g beads after 90 min). The same trend was detected for the antioxidant

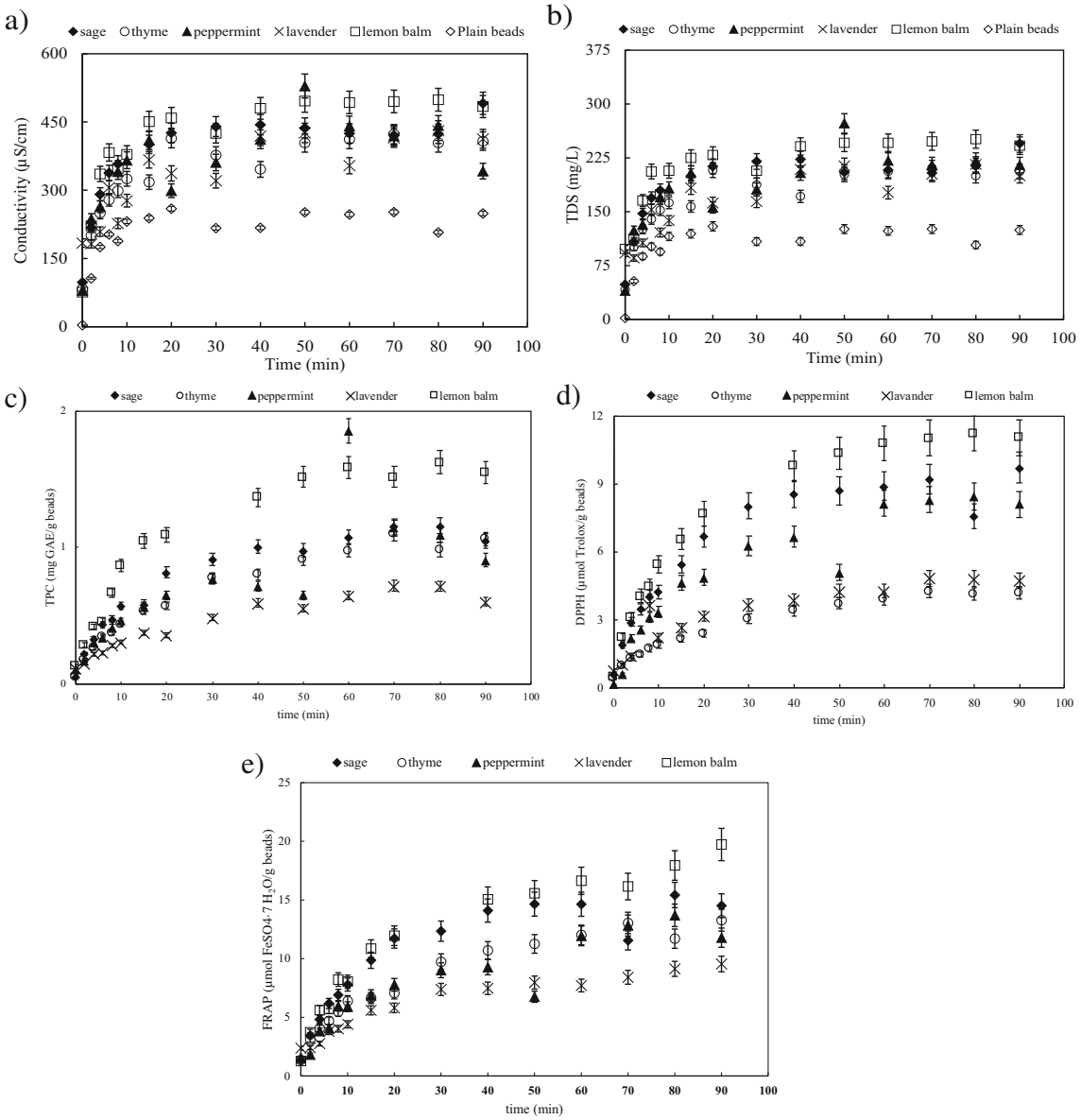

Fig. 3 Release profiles of bioactives from *Lamiaceae* microbeads: (**a**) conductivity, (**b**) TDS, (**c**) TPC, (**d**) DPPH, and (**e**) FRAP. The control experiment is not shown in (c, d, and e) since it did not reveal the presence of TPC and antioxidants in samples

capacity determined by the FRAP method (Fig. 3(e)), while for the DPPH method, thyme showed the lowest values of released bioactives after 90 min (4.1 μmol $FeSO_4 \cdot 7H_2O$/g beads). Also, during the release process, a simultaneous rise of conductivity, total dissolved solids (TDS), polyphenolic (TPC), and antioxidant capacity values in the release media was detected at regular time intervals, which was an indication that the conductometric method can be used to follow the release process of bioactives from microbeads. However, based on the data obtained in this study, its major restriction includes the need for a mandatory calibration based on the release solvent used, if that solvent contains ions which can play a significant role in the conductivity of the media used for release analysis. In case of organic solvents (e.g., ethanol, methanol etc.), calibration would not be needed, but in case of water or polar solvents, calibration would be mandatory. It can be seen from the conductometric and chemical release data that most of the bioactives exit the alginate matrix during first 20 min of the release process, during which the biggest change in the concentration of bioactives in the solvent was detected. After the initial fast release phase, the release is slowed down and the changes in concentrations of bioactives in the solvent are not as pronounced as in the beginning of the process. Also, it can be seen from Fig. 3 (c, d, and e) that the increase of TPC in the release medium is followed by the increase in antioxidant capacities measured by the DPPH and the FRAP method, which confirms that polyphenolic compounds were responsible for the antioxidant effect of the beads. The same was concluded in a study by Stojanović et al. (2012). Release profiles of limonene from microbeads were analyzed by Ansarifar et al. (2017), who also noticed two phases of release: the initial rapid release which happens when the bioactives pass through the pores, and the second, slow release which is governed by diffusion through the microcapsule wall. In extrusion encapsulation, sodium alginate is mostly used as wall material (Grgić et al. 2020), but alginate can also be used in combination with other compounds to regulate the release of the bioactives. Stojanović et al. (2012) compared the release of polyphenols from calcium alginate beads and calcium alginate — inulin beads, where the addition of inulin extended the release to 15 min in comparison to alginate beads, which reached a plateau after 10 min. Belščak-Cvitanović et al. (2011) found that when alginate is used in combination with chitosan, the majority of polyphenols are released during a longer time period — 20 to 30 min. Also, in a study by Giunchedi et al. (2000), the addition of HPMC to alginate enhanced the sustained release by providing a denser inner matrix. Sun et al. (2019) analyzed the release profiles of carvacrol from a pectin-alginate matrix and also concluded that more than 60% of carvacrol was released after first 3 h, while the rest was released after the following 22 h.

Kinetic Analysis of the Release Profiles and Mathematical Modeling

A detailed kinetic analysis of the release profiles is of great importance for understanding the forces which govern the release process. Results of the kinetic analysis based on the concentrations of polyphenols in the release media (water) are shown in Table 4.

Four kinetic models were tested for their adequacy to describe the release of *Lamiaceae* bioactives from microbeads: zero order, first order, Korsmeyer-Peppas, and Higuchi. According to Valinger et al. (2018), a good-fitting model has R^2 values above 0.90 while values between 0.70 and 0.90 indicate that the model(s) is considered fairly precise without significant capacity to be used as a tool for quantitative prediction.

The zero-order kinetic model R^2 values ranged from 0.6060 for peppermint to 0.8759 for thyme, which was an indication that the model cannot be used for quantitative prediction of the release process from the microbeads. Even lower R^2 values were obtained for the first order kinetic model for all plants, which was an indication that the first order kinetic model cannot be used for quantitative prediction either. Markedly higher R^2 values, as well as lower RMSE values, were obtained for the two empirical models: Korsmeyer-Peppas and Higuchi. The Korsmeyer-Peppas model proved to be the best to describe the release of polyphenols (TPC) from plant microbeads, with an exception of the lavender microbeads, where the bioactives release profile followed the Higuchi kinetics, with an emphasis on the fact that the R^2 and the RMSE values were very similar for the Higuchi and the Korsmeyer-Peppas model, within the margin of experimental error. The adequacy of the Higuchi and the Korsmeyer-Peppas empirical models for description of the release processes from microcapsules was also confirmed in a study by Dima et al. (2016), who studied the release of *Coriandrum sativum* L. essential oil from chitosan/alginate/inulin microcapsules, as well as in a study of the release of grape phenolics from spray dried microcapsules by Moreno et al. (2018). It must be emphasized that in those studies, gastric release was modeled. For easier comparison of the release rates and the mechanisms governing the release process, the Korsmeyer-Peppas model parameters will be used in further discussion.

As mentioned earlier, in the Korsmeyer-Peppas model, two parameters can be assessed: the release rate k, which tells us how fast the bioactives exit the microbeads, and the n, which defines which is the prevailing mechanism of release (Rezaei and Nasirpour 2019). The release rate values (k) for TPC ranged from 0.130 ± 0.020 min^{-1} for lavender to 0.326 ± 0.048 min^{-1} for lemon balm microbeads, which indicated that the lemon balm polyphenols entrapped in the alginate matrix were released the fastest. The n values for the release of polyphenols were lower than 0.5 which means that the polyphenols are released from the microbeads following a pseudo-Fickian diffusion mechanism. According to Kuipers and

Table 4 Estimated kinetic parameters for the release process of bioactives from *Lamiaceae* microbeads. Models marked bold are selected for further analyses

	Kinetic model	TPC/ mgGAE/g_{beads}				
		k/ min^{-1}	Mo/ mgGAE/ g_{beads}	n	R^2	RMSE
Sage	Zero order	0.017 ± 0.007	0.48 ± 0.07	**0.36 ± 0.03**	0.7857	0.3065
	First order	0.011 ± 0.002			0.6853	0.1972
	Korsmeyer-Peppas	**0.244 ± 0.028**			**0.9779**	**0.0729**
	Higuchi	0.140 ± 0.005			0.9427	0.1164
Thyme	Zero order	0.015 ± 0.001	0.38 ± 0.05	**0.43 ± 0.02**	0.8759	0.2273
	First order	0.013 ± 0.002			0.8785	0.1583
	Korsmeyer-Peppas	**0.166 ± 0.016**			**0.9896**	**0.0476**
	Higuchi	0.124 ± 0.003			0.9825	0.0617
Peppermint	Zero order	0.016 ± 0.002	0.42 ± 0.10	**0.44 ± 0.12**	0.6060	0.3431
	First order	0.013 ± 0.004			0.7180	0.3002
	Korsmeyer-Peppas	**0.172 ± 0.080**			**0.8194**	**0.2472**
	Higuchi	0.134 ± 0.012			0.8151	0.2498
Lavender	Zero order	0.010 ± 0.001	0.28 ± 0.03	**0.38 ± 0.04**	0.8564	0.1702
	First order	0.012 ± 0.002			0.7618	0.0975
	Korsmeyer-Peppas	**0.130 ± 0.020**			**0.9338**	**0.0535**
	Higuchi	0.082 ± 0.003			0.9429	0.0682
Lemon balm	Zero order	0.023 ± 0.003	0.65 ± 0.10	**0.37 ± 0.04**	0.8026	0.4098
	First order	0.012 ± 0.002			0.7068	0.1049
	Korsmeyer-Peppas	**0.326 ± 0.046**			**0.9468**	**0.1148**
	Higuchi	0.197 ± 0.008			0.9334	0.1613

Beenackers (1993), the diffusion in many polymers (especially the ones prone to swelling) cannot be described adequately by Fick's law because of the time dependency of the properties of a polymer, due to the finite rate of adjustment of the polymer chains to the presence of the penetrant. Also, deviation from the Fick's law can occur due to the size of the entrapped molecule in relation to the mesh size of the polymer (Valério et al. 2019). In this case, the mechanism of release is not completely Fickian, which can be explained by the fact that, besides diffusion, swelling was present in the initial release testing phase. In a release study of curcumin from almond gum/PVA nanofibers by Rezaei and Nasirpour (2019), the release was found to be controlled by anomalous diffusion. In another study performed by Sun et al. (2013), the release of curcumin and curcumin-CD complex from PVA nanofibers was governed by diffusion mechanism and followed the Higuchi kinetics. Furthermore, in a study by Anisafar et al. (2017), release of limonene from multilayer microcapsules was found to follow a non-Fick law and was a combination of diffusion and erosion mechanisms.

Conclusions

In this study, the adsorption and the release of *Lamiaceae* bioactives form alginate beads was analyzed. Based on the analysis of the extract used for the adsorption process, it was concluded that the highest amount of polyphenols (30% of the polyphenols contained in the extract) was transferred to the microbeads from the thyme extract. Also, a period of bead shrinkage during the adsorption process was detected which lasted until 30 min for thyme, 50 min for lavender, lemon balm, and peppermint, while the shrinkage for the sage extract lasted for 60 min. A combination of chemical and conductometric methods can be used to follow the release process of the bioactives, since it follows the rising trends of concentration of the bioactives in the release medium shown by chemical methods. The best suited model for the description of the bioactives' release kinetics was the Korsmeyer-Peppas model and the release was governed by a pseudo-Fickian diffusion mechanism Given the fact that the amounts of bioactives are initially higher in the extracts, and the changes in bioactives concentrations are rather low during the dynamic adsorption/release experiments, monitoring the concentration changes in the extracts proved to be a reliable alternative to monitor such processes.

Author Contribution Maja Benković — designed the analysis, collected the data, revised the manuscript.

Ivana Sarić — collected the data.

Ana Jurinjak Tušek — performed the mathematical modeling, revised the manuscript.

Tamara Jurina — prepared the chart and tables, revised the manuscript.

Jasenka Gajdoš Kljusurić — collected the data, revised the paper.

Davor Valinger — collected the data, wrote the paper.

Data Availability Not applicable.

Code Availability Not applicable.

Declarations

Competing Interests The authors declare no competing interests.

References

Ansarifar, E., Mohebbi, M., Shahidi, F., Koocheki, A., & Ramezanian, N. (2017). Novel multilayer microcapsules based on soy protein isolate fibrils and high methoxyl pectin: Production, characterization and release modeling. *International Journal of Biological Macromolecules, 97*, 761–769. https://doi.org/10.1016/j.ijbiomac.2017.01.056.

Bajpai, S. K., & Sharma, S. (2004). Investigation of swelling/degradation behaviour of alginate beads crosslinked with Ca^{2+} and Ba^{2+} ions. *Reactive and Functional Polymers, 59*(2), 129–140. https://doi.org/10.1016/j.reactfunctpolym.2004.01.002.

Belščak-Cvitanović, A., Stojanović, R., Manojlović, V., Komes, D., Juranović Cindrić, I., Nedović, V., & Bugarski, B. (2011). Encapsulation of polyphenolic antioxidants from medicinal plant extracts in alginate–chitosan system enhanced with ascorbic acid by electrostatic extrusion. *Food Research International, 44*(4), 1094–1101. https://doi.org/10.1016/j.foodres.2011.03.030.

Belščak-Cvitanović, A., Komes, D., Karlović, S., Djakovic, S., Špoljarić, I., Mršić, G., & Ježek, D. (2015). Improving the controlled delivery formulations of caffeine in alginate hydrogel beads combined with pectin, carrageenan, chitosan and psyllium. *Food Chemistry, 167*, 378–386. https://doi.org/10.1016/j.foodchem.2014.07.011.

Belščak-Cvitanović, A., Valinger, D., Benković, M., Jurinjak Tušek, A., Jurina, T., Komes, D., & Gajdoš Kljusurić, J. (2018). Integrated approach for bioactive quality evaluation of medicinal plant extracts using HPLC-DAD, spectrophotometric, near infrared (NIR) spectroscopy and chemometric techniques. *International Journal of Food Properties, 20*(sup3), S2463–S2480. https://doi.org/10.1080/10942912.2017.1373122.

Benzie, I., & Strain, J. (1996). The ferric reducing ability of plasma (FRAP) as a measure of "antioxidant power: The FRAP assay". *Analytical Biochemistry, 239*(1), 70–76. https://doi.org/10.1006/abio.1996.0292.

Bodade, R. G., Bodade, A. G. (2020) Chapter 17 - Microencapsulation of bioactive compounds and enzymes for therapeutic applications, In K. Pal, I. Banerjee, P. Sarkar, D. Kim, W-P. Deng, N. Kumar Dubey, K. Majumder (Eds.). *Biopolymer-Based Formulations*, (pp. 381–404). Amsterdam:Elsevier.

Brand-Williams, W., Cuvelier, M. E., & Berset, C. (1995). Use of free radical method to evaluate antioxidant activity. *LWT-Food Science and Technology, 28*(1), 25–30. https://doi.org/10.1016/S0023-6438(95)80008-5.

Bucurescu, A., Blaga, A. C., Estevinho, B. N., & Rocha, F. (2018). Microencapsulation of curcumin by a spray-drying technique using gum arabic as encapsulating agent and release studies. *Food and Bioprocess Technology, 11*(10), 1795–1806. https://doi.org/10.1007/s11947-018-2140-3.

Bušić, A., Belščak-Cvitanović, A., Vojvodić Cebin, A., Karlović, S., Kovač, V., Špoljarić, I., Mršić, G., & Komes, D. (2018). Structuring new alginate network aimed for delivery of dandelion (*Taraxacum officinale* L.) polyphenols using ionic gelation and new filler materials. *Food Research International, 111*, 244–255. https://doi.org/10.1016/j.foodres.2018.05.034.

Chan, E.-S., Yim, Z.-H., Phan, S.-H., Mansa, R. F., & Ravindra, P. (2010). Encapsulation of herbal extracts through absorption with Ca-alginate hydrogel beads. *Food and Bioproducts Processing, 88*(2–3), 195–201. https://doi.org/10.1016/j.fbp.2009.09.005.

Chen, L., Gnanaraj, C., Arulselvan, P., El-Seedi, H., & Teng, H. (2019). A review on advanced microencapsulation technology to enhance bioavailability of phenolic compounds: Based on its activity in the treatment of type 2 diabetes. *Trends in Food Science & Technology, 85*, 149–162. https://doi.org/10.1016/j.tifs.2018.11.026.

Cortés-Camargo, S., Acuña-Avila, P. E., Rodríguez-Huezo, M. E., Román-Guerrero, A., Varela-Guerrero, V., & Pérez-Alonso, C. (2019). Effect of chia mucilage addition on oxidation and release kinetics of lemon essential oil microencapsulated using mesquite gum – Chia mucilage mixtures. *Food Research International, 116*, 1010–1019. https://doi.org/10.1016/j.foodres.2018.09.040.

Dima, C., Pătraşcu, L., Cantaragiu, A., Alexe, P., & Dima, S. (2016). The kinetics of the swelling process and the release mechanisms of *Coriandrum sativum* L. essential oil from chitosan/alginate/inulin microcapsules. *Food Chemistry, 195*, 39–48. https://doi.org/10.1016/j.foodchem.2015.05.044.

Dominguez, M. A., Etcheverry, M., & Zanini, G. P. (2019). Evaluation of the adsorption kinetics of brilliant green dye onto a montmorillonite/alginate composite beads by the shrinking core model. *Adsorption, 25*(7), 1387–1396. https://doi.org/10.1007/s10450-019-00101-w.

Dorman, H. J. D., Peltoketo, A., Hiltunen, R., & Tikkanen, M. J. (2003). Characterisation of the antioxidant properties of de-odourised aqueous extracts from selected Lamiaceae herbs. *Food Chemistry, 83*(2), 255–262. https://doi.org/10.1016/S0308-8146(03)00088-8.

Fangmeier, M., Lehn, D. N., Maciel, M. J., & de Souza, C. F. V. (2019). Encapsulation of bioactive ingredients by extrusion with vibrating technology: Advantages and challenges. *Food and Bioprocess Technology, 12*(9), 1472–1486. https://doi.org/10.1007/s11947-019-02326-7.

Fornari, T., Ruiz-Rodriguez, A., Vicente, G., Vázquez, E., García-Risco, M. R., & Reglero, G. (2012). Kinetic study of the supercritical CO_2 extraction of different plants from *Lamiaceae* family. *The Journal of Supercritical Fluids, 64*, 1–8. https://doi.org/10.1016/j.supflu.2012.01.006.

Giunchedi, P., Gavini, E., Moretti, M. D. L., & Pirisino, G. (2000). Evaluation of alginate compressed matrices as prolonged drug delivery systems. *AAPS PharmSciTech, 1*(3), 19–36. https://doi.org/10.1208/pt010319.

Gonçalves, B., Moeenfard, M., Rocha, F., Alves, A., Estevinho, B. N., & Santos, L. (2017). Microencapsulation of a natural antioxidant from coffee—Chlorogenic acid (3-caffeoylquinic acid). *Food and Bioprocess Technology, 10*(8), 1521–1530. https://doi.org/10.1007/s11947-017-1919-y.

Grgić, J., Šelo, G., Planinić, M., Tišma, M., & Bucić-Kojić, A. (2020). Role of the encapsulation in bioavailability of phenolic compounds. *Antioxidants, 2020*(9), 923. https://doi.org/10.3390/antiox9100923.

Jim, Z. H., Tiong, C. B., Mansa, R. F., Ravindra, P., & Chan, E. S. (2010). Release kinetics of encapsulated herbal antioxidants during gelation process. *Journal of Applied Science, 10*(21), 2668–2672. https://doi.org/10.3923/jas.2010.2668.2672.

Jurinjak Tušek, A., Benković, M., Belščak Cvitanović, A., Valinger, D., Jurina, T., & Gajdoš Kljusurić, J. (2016). Kinetics and thermodynamics of the solid-liquid extraction process of total polyphenols, antioxidants and extraction yield from *Asteraceae* plants. *Industrial Crops and Products, 91*, 205–214. https://doi.org/10.1016/j.indcrop.2016.07.015.

Jurinjak Tušek, A., Benković, M., Valinger, D., Jurina, T., Belščak-Cvitanović, A., & Gajdoš Kljusurić, J. (2018). Optimizing bioactive compounds extraction from different medicinal plants and prediction through nonlinear and linear models. *Industrial Crops and Products, 126*, 449–458. https://doi.org/10.1016/j.indcrop.2018.10.040.

Jurinjak Tušek, A., Jurina, T., Benković, M., Valinger, D., Belščak-Cvitanović, A., & Jasenka Gajdoš Kljusurić, J. (2020). Application of multivariate regression and artificial neural network modelling for prediction of physical and chemical properties of medicinal plants aqueous extracts. *Journal of Applied Research on Medicinal and Aromatic Plants, 16*, 100229. https://doi.org/10.1016/j.jarmap.2019.100229.

Kuipers, N. J. M., & Beenackers, A. A. C. M. (1993). Non-fickian diffusion with chemical reaction in glassy polymers with swelling induced by the penetrant: A mathematical model. *Chemical Engineering Science, 48*(16), 2957–2971. https://doi.org/10.1016/0009-2509(93)80041-N.

Lee, K. Y., & Mooney, D. J. (2012). Alginate: Properties and biomedical applications. *Progress in Polymer Science, 37*(1), 106–126. https://doi.org/10.1016/j.progpolymsci.2011.06.003.

Marchioni, I., Najar, B., Ruffoni, B., Copetta, A., Pistelli, L., & Pistelli, L. (2020). Bioactive compounds and aroma profile of some Lamiaceae edible flowers. *Plants, 9*(6), 691. https://doi.org/10.3390/plants9060691.

Massounga Bora, A. F., Ma, S., Li, X., & Liu, L. (2018). Application of microencapsulation for the safe delivery of green tea polyphenols in food systems: Review and recent advances. *Food Research International, 105*, 241–249. https://doi.org/10.1016/j.foodres.2017.11.047.

Matkowski, A., & Piotrowska, M. (2006). Antioxidant and free radical scavenging activities of some medicinal plants from the Lamiaceae. *Fitoterapia, 77*(5), 346–353. https://doi.org/10.1016/j.fitote.2006.04.004.

Montanucci, P., Terenzi, S., Santi, C., Pennoni, I., Binni, V., Pescara, T., Basta, G., & Calafiore, R. (2015). Insights in behaviour of variably formulated alginate-based microcapsules for cell transplantation. *BioMed Research International, 2015*, 965804–965811. https://doi.org/10.1155/2015/965804.

Moreno, T., Cocero, M. J., & Rodriguez-Rojo, S. (2018). Storage stability and simulated gastrointestinal release of spray dried grape marc phenolics. *Food and Bioproducts Processing, 112*, 96–107. https://doi.org/10.1016/j.fbp.2018.08.011.

Obidike, I. C., & Emeje, M. O. (2011). Microencapsulation enhances the anti-ulcerogenic properties of *Entada africana* leaf extract. *Journal of Ethnopharmacology, 137*(1), 553–561. https://doi.org/10.1016/j.jep.2011.06.012.

Oreopoulou, A., Papavassilopoulou, E., Bardouki, H., Vamvakias, M., Bimpilas, A., & Oreopoulou, V. (2018). Antioxidant recovery from hydrodistillation residues of selected Lamiaceae species by alkaline extraction. *Journal of Applied Research on Medicinal and Aromatic Plants, 8*, 83–89. https://doi.org/10.1016/j.jarmap.2017.12.004.

Pham, V. T., & Fulton, J. L. (2013). Ion-pairing in aqueous $CaCl_2$ and RbBr solutions: Simultaneous structural refinement of XAFS and XRD data. *The Journal of Chemical Physics, 138*(4), 044201. https://doi.org/10.1063/1.4775588.

Puscaselu, R. G., Lobius, A., Dimian, M., & Covasa, M. (2020). Alginate: From food industry to biomedical applications and management of metabolic disorders. *Polymers, 2020*(12), 2417. https://doi.org/10.3390/polym12102417.

Rezaei, A., & Nasirpour, A. (2019). Evaluation of release kinetics and mechanisms of curcumin and curcumin-β-cyclodextrin inclusion complex incorporated in electrospun almond gum/pva nanofibers in simulated saliva and simulated gastrointestinal conditions. *Bio Nano Sci., 9*(2), 438–445. https://doi.org/10.1007/s12668-019-00620-4.

Rodrigues, D., Sousa, S., Gomes, A. M., Pintado, M. M., Silva, J. P., Costa, P., Amral, M. H., Rocha-Santos, T., & Freitas, A. C. (2012). Storage stability of *Lactobacillus paracasei* as free cells or encapsulated in alginate-based microcapsules in low pH fruit juices. *Food and Bioprocess Technology, 5*(7), 2748–2757. https://doi.org/10.1007/s11947-011-0581-z.

Rusydi, A.F. (2018). Correlation between conductivity and total dissolved solid in various type of water: a review. *IOP Conf. Series: Earth and Environmental Science 118,* 012019, https://doi.org/10.1088/1755-1315/118/1/012019.

Saad, R., Asmani, F., Saad, M., Hussain, M., Khan, J., Kaleemullah, M., Othman, N. B., Tofigh, A., & Yusuf, E. (2015) A new approach for predicting antioxidant property of herbal extracts. *International Journal of Pharmacognosy and Phytochemical Research, 7*(1), 166–174.

Saitoh, S., Araki, Y., Kon, R., Katsura, H., & Taira, M. (2000). Swelling/deswelling mechanism of calcium alginate gel in aqueous solutions. *Dental Materials Journal, 19*(4), 396–404. https://doi.org/10.4012/dmj.19.396.

Shinde, T., Sun-Waterhouse, D., & Brooks, J. (2014). Co-extrusion encapsulation of probiotic *Lactobacillus acidophilus* alone or together with apple skin polyphenols: An aqueous and value-added delivery system using alginate. *Food and Bioprocess Technology, 7*(6), 1581–1596. https://doi.org/10.1007/s11947-013-1129-1.

Singleton, V. L., & Rossi, J. A. (1965). Colorimetry of total phenolics with phosphomolybdic-phosphotungstic acid reagents. *American Journal of Enology and Viticulture, 16*, 144–158.

Skendi, A., Irakli, M., & Chatzopoulou, P. (2017). Analysis of phenolic compounds in Greek plants of Lamiaceae family by HPLC. *Journal of Applied Research on Medicinal and Aromatic Plants, 6*, 62–69. https://doi.org/10.1016/j.jarmap.2017.02.001.

Stojanović, R., Belščak-Cvitanović, A., Manojlović, V., Komes, D., Nedović, V., & Bugarski, B. (2012). Encapsulation of thyme (*Thymus serpyllum* L.) aqueous extract in calcium alginate beads. *Journal of the Science of Food and Agriculture, 92*(3), 685–696. https://doi.org/10.1002/jsfa.4632.

Strobel, S. A., Scher, H. B., Nitin, N., & Jeoh, T. (2016). In situ cross-linking of alginate during spray-drying to microencapsulate lipids in powder. *Food Hydrocolloids, 58*, 141–149. https://doi.org/10.1016/j.foodhyd.2016.02.031.

Strobel, S. A., Hudnall, K., Arbaugh, B., Cunniffe, J. C., Scher, H. B., & Jeoh, T. (2020). Stability of fish oil in calcium alginate microcapsules cross-linked by in situ internal gelation during spray drying. *Food and Bioprocess Technology, 13*(2), 275–287. https://doi.org/10.1007/s11947-019-02391-y.

Sudar, M., Findrik, Z., Szekrenyi, A., Clapés, P., & Vasić-Rački, Đ. (2019). Reactor and microreactor performance and kinetics of the aldol addition of dihydroxyacetone to benzyloxycarbonyl-N-3-aminopropanal catalyzed by D-fructose-6-phosphate aldolase variant A129G. *Chemical Engineering Communications, 206*(7), 927–939. https://doi.org/10.1080/00986445.2018.1538975.

Sun, X., Williams, G., Hou, X., & Zhu, L. (2013). Electrospun curcumin-loaded fibers with potential biomedical applications. *Carbohydrate polymer, 94*(1), 147–153. https://doi.org/10.1016/j.carbpol.2012.12.064.

Sun, X., Cameron, R. G., & Bai, J. (2019). Microencapsulation and antimicrobial activity of carvacrol in a pectin-alginate matrix. *Food Hydrocolloids, 92*, 69–73. https://doi.org/10.1016/j.foodhyd.2019.01.006.

Tarone, A. G., Cazarin, C. B. B., & Junior, M. R. M. (2020). Anthocyanins: New techniques and challenges in microencapsulation. *Food Research International, 133*, 109092. https://doi.org/10.1016/j.foodres.2020.109092.

Valério, A., Mancusi, E., Ferreira, F., Guelli Ulson de Souza, S. M. A., Ulson de Souza, A. A., & Gómez González, S. Y. (2019). Biopolymer-hydrophobic drug fibers and the delivery mechanisms

for sustained release applications. *European Polymer Journal, 112*, 400–410. https://doi.org/10.1016/j.eurpolymj.2019.01.016.

Valinger, D., Kušen, M., Jurinjak Tušek, A., Panić, M., Jurina, T., Benković, M., Radojčić Redovniković, I., & Gajdoš Kljusurić, J. (2018). Development of near infrared spectroscopy models for quantitative prediction of the content of bioactive compounds in olive leaves. *Chemical and Biochemical Engineering Quarterly, 32*, 535–543. https://doi.org/10.15255/CABEQ.2018.1396.